SICE Annual Conference 2014
September 9-12, 2014, Hokkaido University, Sapporo, Japan

Intelligent Second-Order Sliding-Mode Control for Chaotic Tracking Problem

Chun-Fei Hsu[1], Tsu-Tian Lee[2] and Chun-Wei Chang[1]

[1] Department of Electrical Engineering, Tamkang University, New Taipei City, Taiwan
(Tel : +886-2-2621-5656; E-mail: fei@ee.tku.edu.tw; 601460214@s01.tku.edu.tw)
[2] Department of Electrical Engineering, Chung Yuan Christian University, Chung Li, Taiwan
(Tel : +886-3-265-9999; E-mail: ttlee@cycu.edu.tw)

Abstract: The behavior of a chaotic dynamic system is extremely sensitive to the system parameters and initial conditions. In this paper, a recurrent fuzzy neural network (RFNN) is used to online approximate the unknown nonlinear term of chaotic system dynamics with a good accuracy. Meanwhile, an intelligent second-order sliding-mode control (ISSMC) system is proposed for a chaotic dynamic system with high accuracy tracking response. A neural controller and a robust compensator are designed in the proposed ISSMC system. Because of the ISSMC system uses integration method to obtain the actual control signal, the chattering phenomenon can be removed effectively. Further, the controller parameter adaptation laws are derived based on the Lyapunov function, so that the system stability of the closed-loop system can be guaranteed. Finally, the proposed ISSMC method is successfully applied to the chaotic tracking control problem.

Keywords: neural network control, sliding-mode control, recurrent fuzzy neural network, Lyapunov function.

1. INTRODUCTION

During the past four decades, sliding mode control (SMC) is a popular robust strategy to treat uncertain control systems [1, 2]. The important feature of the SMC scheme is its ability to deal with external disturbances and unmodeled system dynamics. The SMC has other advantages liking as ease of implementation and reduction in the order of the state equation. Such properties make the SMC system suitable for real-time control applications for nonlinear dynamic control systems. However, to satisfy the sliding condition, a switching control law should be constructed, which results in the chattering phenomena. However, the chattering phenomenon is a well-known disadvantage of the SMC method.

To attack this problem, several methods have been proposed to solve the chattering problem. A common method is using a saturation function to replace a switching function in the switching control law [2]. But, an indefinite steady state error will be caused if the boundary layer is selected too large. Another method is to diminish the gain of the switching control law. If the switching control law is not strong enough to deal with the system uncertainties, the robustness of the SMC system will become poor.

For the chattering eliminating, a second-order sliding-mode control (SSMC) is an effective method [3, 4]. A discontinuous switching control law is contained in the derivative control signal and the actual control signal is obtained after integrating the discontinuous switching control law. Thus, the SSMC system possesses the advantages of system stability, without chattering and system robustness to uncertainties which are usually composed of unpredictable plant parameter variations and external disturbances.

On the other hand, various intelligent sliding-mode controllers of nonlinear systems using fuzzy system, neural network or neural-fuzzy approaches have been proposed [5-11]. Especially when systems have large uncertainties and strong nonlinearities, it is known that fuzzy systems, neural networks or neural-fuzzy systems are powerful techniques in the discipline of system control and system description. For real-time practical implementation, the controller parameters of the intelligent sliding-mode controller can be online tuned by the online parameter learning algorithm, but it doest not require off-line parameter learning algorithm.

The fuzzy neural network (FNN) possesses both of the advantages of fuzzy systems and neural networks. It brings the learning and computational power of neural networks into fuzzy systems and provides the human thinking and reasoning of fuzzy systems into neural networks [12, 13]. However, the FNN applications are limited to the static input-output mapping problems due to that FNNs are feedforward neural network. To attack this problem, interest in using a recurrent fuzzy neural network (RFNN) has been steadily growing [14-18]. Un-liking the FNN, RFNN demonstrates good control performance in the presence of system uncertainties due to the RFNN has feedback loops which are used to memorize past information [18].

The purpose of this paper proposes an intelligent second-order sliding-mode control (ISSMC) system, which combining the principles of SSMC and RFNN, for a chaotic tracking control problem. A RFNN is used to online approximate the unknown nonlinear term of chaotic dynamics systems with a good accuracy. Meanwhile, a parameter learning algorithm is derived in the sense of a Lyapunov function to guarantee system stable. Finally, the simulation results verify that the system stabilization, system robustness and favorable tracking performance can be achieved by the proposed ISSMC system.

2. DESCRIPTION OF RFNN

The network structure of RFNN is given as shown in Fig. 1, where there are two input variables and one

output variable. The operation functions in each layer are introduced in the following.

Layer 1: No function is performed in this layer.

Layer 2: Each node in this layer defines a Gaussian membership function. For the *i*-th input, the function is given as

$$\varphi_{ij} = \exp\left(-\frac{1}{2}\left(\frac{x_i - c_{ij}}{v_{ij}} \right)^2 \right), \text{ for } \; j = 1,2,...,n \qquad (1)$$

where n is the number of fuzzy sets and v_{ij} and c_{ij} are the adjustable parameters.

Layer 3: The firing strength of the *k*-th rule is

$$\phi_k = \prod_{i=1}^{2} \varphi_{ij} \text{ , for } \; k = 1,2,...,m \qquad (2)$$

where m is the number of fuzzy rules.

Layer 4: The temporal firing strength is a linear combination function expressed as

$$\Theta_o = \phi_o + \sum_{k=1}^{m} r_{ko} \Theta_k^{pre} \text{ , for } \; o = 1,2,...,m \qquad (3)$$

where r_{ko} is the recurrent weight of the *k*-th recurrent neuron to *o*-th recurrent neuron and Θ_k^{pre} is the output signals of the *k*-th recurrent neuron in the previous time.

Layer 5: The output is obtained as

$$y = \sum_{o=1}^{m} \alpha_j \Theta_j = \boldsymbol{\alpha}^T \boldsymbol{\Theta}(\mathbf{c}, \mathbf{v}, \mathbf{r}) = \boldsymbol{\alpha}^T \boldsymbol{\Theta} \qquad (4)$$

where $\boldsymbol{\alpha} = [\alpha_1,...,\alpha_m]^T$, $\boldsymbol{\Theta} = [\Theta_1,...,\Theta_m]^T$, $\mathbf{c} = [c_{11}, c_{21},..., c_{1m}, c_{2m}]^T$, $\mathbf{v} = [v_{11}, v_{21},..., v_{1m}, v_{2m}]^T$ and $\mathbf{r} = [r_{11},..., r_{m1},..., r_{1m}, r_{mm}]^T$.

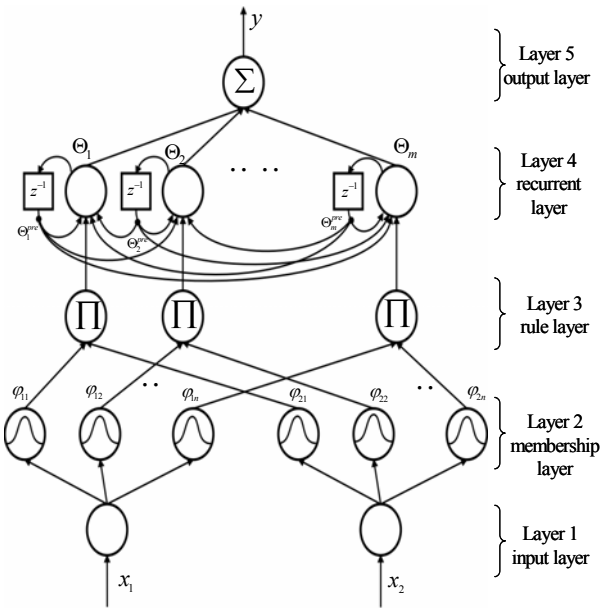

Fig. 1. Network structure of RFNN.

By the universal function approximation of RFNN, it implies that there exists an ideal RFNN y^* such that it can approximate a time-varying nonlinear function Ω as [18]

$$\Omega = y^* + \Delta = \boldsymbol{\alpha}^{*T} \boldsymbol{\Theta}(\mathbf{c}^*, \mathbf{v}^*, \mathbf{r}^*) + \Delta = \boldsymbol{\alpha}^{*T} \boldsymbol{\Theta}^* + \Delta \qquad (5)$$

where $\boldsymbol{\alpha}^*$ and $\boldsymbol{\Theta}^*$ are the optimal parameter vectors of $\boldsymbol{\alpha}$ and $\boldsymbol{\Theta}$, respectively, $\mathbf{c}^*$, $\mathbf{v}^*$ and $\mathbf{r}^*$ are those of $\mathbf{c}$, $\mathbf{v}$ and $\mathbf{r}$, respectively, and Δ is the approximation error. And, an estimated RFNN $\hat{y}$ is given as

$$\hat{y} = \hat{\boldsymbol{\alpha}}^T \boldsymbol{\Theta}(\hat{\mathbf{c}}, \hat{\mathbf{v}}, \hat{\mathbf{r}}) = \hat{\boldsymbol{\alpha}}^T \hat{\boldsymbol{\Theta}} \qquad (6)$$

where $\hat{\boldsymbol{\alpha}}$ and $\hat{\boldsymbol{\Theta}}$ are the estimates of $\boldsymbol{\alpha}^*$ and $\boldsymbol{\Theta}^*$, respectively, and $\hat{\mathbf{c}}$, $\hat{\mathbf{v}}$ and $\hat{\mathbf{r}}$ are those of $\mathbf{c}^*$, $\mathbf{v}^*$ and $\mathbf{r}^*$, respectively. Thus, the estimation error can be obtained as

$$\tilde{y} = \Omega - \hat{y} = \tilde{\boldsymbol{\alpha}}^T \hat{\boldsymbol{\Theta}} + \hat{\boldsymbol{\alpha}}^T \tilde{\boldsymbol{\Theta}} + \tilde{\boldsymbol{\alpha}}^T \tilde{\boldsymbol{\Theta}} + \Delta \qquad (7)$$

where $\tilde{\boldsymbol{\alpha}} = \boldsymbol{\alpha}^* - \hat{\boldsymbol{\alpha}}$ and $\tilde{\boldsymbol{\Theta}} = \boldsymbol{\Theta}^* - \hat{\boldsymbol{\Theta}}$. Taking the Taylor series expansion of $\tilde{\boldsymbol{\Theta}}$ to obtain [8, 9]

$$\tilde{\boldsymbol{\Theta}} = \mathbf{A}^T \tilde{\mathbf{c}} + \mathbf{B}^T \tilde{\mathbf{v}} + \mathbf{C}^T \tilde{\mathbf{r}} + \mathbf{h} \qquad (8)$$

where $\tilde{\mathbf{c}} = \mathbf{c}^* - \hat{\mathbf{c}}$ $\tilde{\boldsymbol{\sigma}} = \boldsymbol{\sigma}^* - \hat{\boldsymbol{\sigma}}$ $\tilde{\mathbf{r}} = \mathbf{r}^* - \hat{\mathbf{r}}$,

$\mathbf{A} = \left[\frac{\partial \Theta_1}{\partial \mathbf{c}} \;\; \cdots \;\; \frac{\partial \Theta_m}{\partial \mathbf{c}} \right]\Big|_{\mathbf{c}=\hat{\mathbf{c}}}$, $\mathbf{B} = \left[\frac{\partial \Theta_1}{\partial \mathbf{v}} \;\; \cdots \;\; \frac{\partial \Theta_m}{\partial \mathbf{v}} \right]\Big|_{\mathbf{v}=\hat{\mathbf{v}}}$,

$\mathbf{C} = \left[\frac{\partial \Theta_1}{\partial \mathbf{r}} \;\; \cdots \;\; \frac{\partial \Theta_m}{\partial \mathbf{r}} \right]\Big|_{\mathbf{r}=\hat{\mathbf{r}}}$, and $\mathbf{h}$ is a vector containing high order terms. Substituting (8) into (7) yields

$$\tilde{y} = \tilde{\boldsymbol{\alpha}}^T \hat{\boldsymbol{\Theta}} + \hat{\boldsymbol{\alpha}}^T (\mathbf{A}^T \tilde{\mathbf{c}} + \mathbf{B}^T \tilde{\mathbf{v}} + \mathbf{C}^T \tilde{\mathbf{r}} + \mathbf{h}) + \tilde{\boldsymbol{\alpha}}^T \tilde{\boldsymbol{\Theta}} + \Delta$$

$$= \tilde{\boldsymbol{\alpha}}^T \hat{\boldsymbol{\Theta}} + \tilde{\mathbf{c}}^T \mathbf{A} \hat{\boldsymbol{\alpha}} + \tilde{\mathbf{v}}^T \mathbf{B} \hat{\boldsymbol{\alpha}} + \tilde{\mathbf{r}}^T \mathbf{C} \hat{\boldsymbol{\alpha}} + \varepsilon \qquad (9)$$

where $\varepsilon = \hat{\boldsymbol{\alpha}}^T \mathbf{h} + \tilde{\boldsymbol{\alpha}}^T \tilde{\boldsymbol{\Theta}} + \Delta$ denotes a lumped approximation error. In this paper, a assumption is given as $|\varepsilon| \le E$ where E is a positive constant.

3. ISSMC SYSTEM FOR CHAOTIC TRACKING

3.1 Description of chaotic dynamic

The behavior of a chaotic dynamic system is extremely sensitive to the system parameters and initial conditions applied [19-21]. In the last three decades, control and synchronization of chaotic dynamic systems have become an important topic. This paper considers a Duffing's chaotic dynamic system as [19]

$$\ddot{x} = -p\dot{x} - p_1 x - p_2 x^3 + q\cos(\omega t) + u$$
$$= f(\mathbf{x}) + u \qquad (10)$$

where t is the time variable, $\mathbf{x} = [x, \dot{x}]^T$ is the state vector, ω is the frequency, $f(\mathbf{x})$ is the system

dynamic, u is the control input and p, p_1, p_2 and q are real constants. The open-loop chaotic behavior is simulated with $p=0.4$, $p_1=-1.1$, $p_2=1.0$. In this paper, consider the effect of the system parameters, two simulation cases of the system parameters are considered with Case 1 $(q,\omega)=(1.5,1.6)$ and Case 2 $(q,\omega)=(4.1,1.8)$. The uncontrolled chaotic responses ($u=0$) with initial condition $(x,\dot{x})=(0,0)$ are shown in Fig. 2(a) for Case 1 and in Fig. 2(b) for Case 2. It is shown that the uncontrolled chaotic dynamic system has different chaotic trajectories for different system parameter values.

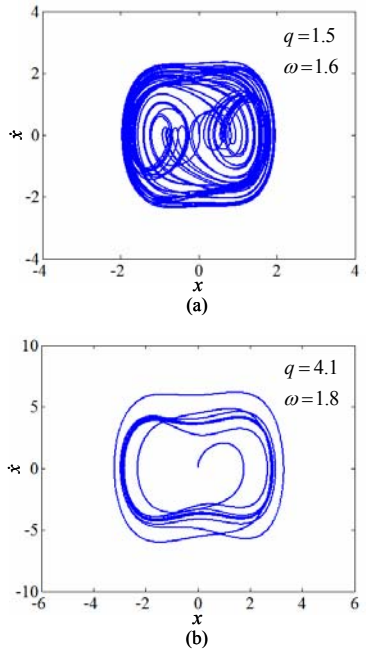

Fig. 2. Behavior of uncontrolled chaotic dynamic.

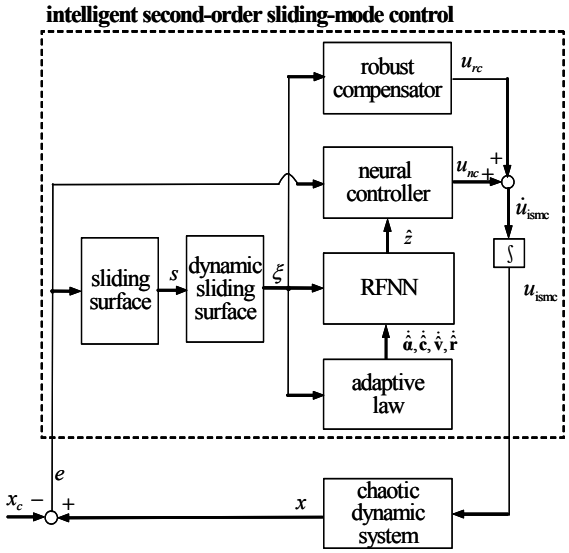

Fig. 3. The block diagram of the ISSMC system.

3.2 Design of ISSMC

The control objective of the chaotic tracking problem is to find a control law so that the chaotic state x can track a chaotic command x_c closely. Define the tracking error as

$$e = x - x_c \tag{11}$$

For controller design, a sliding surface and a dynamic sliding surface are selected as [22-24]

$$s = \dot{e} + a_1 e + a_2 \int_0^t e\,d\tau \tag{12}$$

$$\xi = \dot{s} + b_1 s + b_2 \int_0^t s\,d\tau \tag{13}$$

where a_1, a_2, b_1 and b_2 are positive constants. Differentiating (13) with respect to time and using (12), we can obtain

$$\begin{aligned}\dot{\xi} &= \ddot{s} + b_1\dot{s} + b_2 s \\ &= z(\mathbf{x}) + \dot{u} + c_1\ddot{e} + c_2\dot{e} + c_3 e + c_4\int_0^t e\,d\tau \le 0\end{aligned} \tag{14}$$

where the nonlinear term $z(\mathbf{x}) = \dot{f}(\mathbf{x}) - x_c^{(3)}$, $c_1 = a_1 + b_1$, $c_2 = a_2 + a_1 b_1 + b_2$, $c_3 = a_2 b_1 + a_1 b_2$ and $c_4 = a_2 b_2$. The output of the proposed ISSMC system as shown in Fig. 3 is designed as

$$u_{\text{ismc}} = \int_0^t \dot{u}_{\text{ismc}}\,d\tau \tag{15}$$

$$\dot{u}_{\text{ismc}} = -\hat{z} - c_1\ddot{e} - c_2\dot{e} - c_3 e - c_4\int_0^t e\,d\tau + u_{rc} \tag{16}$$

where $u_{nc} = -\hat{z} - c_1\ddot{e} - c_2\dot{e} - c_3 e - c_4\int_0^t e\,d\tau$ serves as the neural controller, the RFNN output $\hat{z}$ is utilized to online approximate the nonlinear term $z(\mathbf{x})$, and the robust compensator u_{rc} is designed to deal with the effect of the approximation error between $z(\mathbf{x})$ and $\hat{z}$. Imposing the control law $\dot{u} = \dot{u}_{\text{ismc}}$ into (14), we can obtain that

$$\dot{\xi} = z(\mathbf{x}) - \hat{z} + u_{rc} = \tilde{z} + u_{rc} \tag{17}$$

where $\tilde{z} = z(\mathbf{x}) - \hat{z}$. Using the universal function approximation, (17) can be rewritten as

$$\dot{\xi} = \tilde{\boldsymbol{\alpha}}^T\hat{\boldsymbol{\Theta}} + \tilde{\mathbf{c}}^T\mathbf{A}\hat{\boldsymbol{\alpha}} + \tilde{\mathbf{v}}^T\mathbf{B}\hat{\boldsymbol{\alpha}} + \tilde{\mathbf{r}}^T\mathbf{C}\hat{\boldsymbol{\alpha}} + \varepsilon + u_{rc} \tag{18}$$

To prove the stability of the ISSMC system, define a Lyapunov function as

$$V(t) = \frac{1}{2}\xi^2 + \frac{\tilde{\boldsymbol{\alpha}}^T\tilde{\boldsymbol{\alpha}}}{2\eta_\alpha} + \frac{\tilde{\mathbf{c}}^T\tilde{\mathbf{c}}}{2\eta_c} + \frac{\tilde{\mathbf{v}}^T\tilde{\mathbf{v}}}{2\eta_v} + \frac{\tilde{\mathbf{r}}^T\tilde{\mathbf{r}}}{2\eta_r} \tag{19}$$

where η_α, η_c, η_v and η_r are positive learning constants. Differentiating (19) with respect to time and using (18) obtains

$$\dot{V}(t) = \xi\dot{\xi} - \frac{\tilde{\boldsymbol{\alpha}}^T\dot{\hat{\boldsymbol{\alpha}}}}{\eta_\alpha} - \frac{\tilde{\mathbf{c}}^T\dot{\hat{\mathbf{c}}}}{\eta_c} - \frac{\tilde{\mathbf{v}}^T\dot{\hat{\mathbf{v}}}}{\eta_v} - \frac{\tilde{\mathbf{r}}^T\dot{\hat{\mathbf{r}}}}{\eta_r}$$

$$= \tilde{\boldsymbol{\alpha}}^T(\xi\hat{\boldsymbol{\Theta}} - \frac{\dot{\hat{\boldsymbol{\alpha}}}}{\eta_\alpha}) + \tilde{\mathbf{c}}^T(\xi\mathbf{A}\hat{\boldsymbol{\alpha}} - \frac{\dot{\hat{\mathbf{c}}}}{\eta_c}) + \tilde{\mathbf{v}}^T(\xi\mathbf{B}\hat{\boldsymbol{\alpha}} - \frac{\dot{\hat{\mathbf{v}}}}{\eta_v})$$

$$+ \tilde{\mathbf{r}}^T(\xi\mathbf{C}\hat{\boldsymbol{\alpha}} - \frac{\dot{\hat{\mathbf{r}}}}{\eta_r}) + \xi(\varepsilon + u_{rc}). \quad (20)$$

If the parameter adaptive laws are selected as

$$\dot{\hat{\boldsymbol{\alpha}}} = \eta_\alpha \xi \hat{\boldsymbol{\Theta}} \quad (21)$$

$$\dot{\hat{\mathbf{c}}} = \eta_c \xi \mathbf{A}\hat{\boldsymbol{\alpha}} \quad (22)$$

$$\dot{\hat{\mathbf{v}}} = \eta_v \xi \mathbf{B}\hat{\boldsymbol{\alpha}} \quad (23)$$

$$\dot{\hat{\mathbf{r}}} = \eta_r \xi \mathbf{C}\hat{\boldsymbol{\alpha}} \quad (24)$$

and the robust compensator is designed as

$$u_{rc} = -\frac{E}{\delta + (1-\delta)e^{-|\xi|}}\operatorname{sgn}(\xi) \quad (25)$$

where δ is a strictly positive constant that is less than one, then (20) can be rewritten as

$$\dot{V}(t) = \varepsilon\xi - \frac{E}{\delta + (1-\delta)e^{-|\xi|}}|\xi|$$

$$\le |\varepsilon||\xi| - \frac{E}{\delta + (1-\delta)e^{-|\xi|}}|\xi|$$

$$\le E|\xi| - \frac{E}{\delta + (1-\delta)e^{-|\xi|}}|\xi|$$

$$= -(\frac{E}{\delta + (1-\delta)e^{-|\xi|}} - E)|\xi| \le 0 \quad (26)$$

It has been observed that is $\xi \to 0$ as $t \to \infty$ [25]. Thus, the control law of the ISSMC system can guarantee the stability. Meanwhile, if the condition $\xi = 0$ satisfies, the sliding surface convergence to zero ($s = 0$) for all time. It implies that the tracking error convergence to zero ($e = 0$).

Remark 1: Generally speaking, one neural approximator is used under the direct-type intelligent control scheme, but two neural approximators are required to approximate the unknown system dynamics under the indirect-type intelligent control scheme. The proposed ISSMC system is of the indirect type, but it is worth noting that we need only one RFNN to online estimate the nonlinear term.

Remark 2: It can been observed that the control gain of the robust compensator $\frac{E}{\delta + (1-\delta e^{-|\xi|})}$ varies between E and $\frac{E}{\delta}$.

4. SIMULATION RESULTS

It should be emphasized that we does not need to know any knowledge of the chaotic dynamics to construct the proposed ISSMC system. The control parameters of the ISSMC system are selected as $a_1 = b_1 = 4$, $a_2 = b_2 = 4$, $\eta_\alpha = 20$, $\eta_c = \eta_v = \eta_r = 1$, $\delta = 0.5$ and $E = 0.1$. These parameters are selected through some trials. The parameters η_α , η_c , η_v and η_r are the leaning rates in the RFNN. In general, if the leaning rates are chosen to be sufficiently small, this will result in slow learning speed. On the contrary, if the leaning rates are chosen too large, the learning speed can be increased; yet, the system may become unstable. Meanwhile, if the bound constant of approximator error E is not strong enough to deal with the approximator error, the robustness of the ISSMC system will become poor.

In the simulation, the RFNN has two input variables (ξ and ξ) and one output variable ($\hat{z}$) with $3 \times 3 = 9$ fuzzy rules. The simulation results of the ISSMC system are shown in Figs. 4 and 5 for Case 1 and 2, respectively. Since the control rules are initialized from zero ($\boldsymbol{\alpha} = \mathbf{0}$), the RFNN has the drawback of large transient responses of the state trajectories and control efforts during the control parameter learning process. From the simulation results, it shows that the proposed ISSMC system can achieve favorable chaotic tracking responses. Meanwhile, the learned RFNN can online approximate the unknown nonlinear term with a good accuracy.

5. CONCLUSION

Standard second-order sliding-mode control (SSMC) systems in [3, 4] have the main drawback that the control law require the nominal plant model. To avoid the above disadvantage, this paper studies a model-free intelligent second-order sliding-mode control (ISSMC) for a chaotic tracking problem. The behavior of a chaotic system can be evaluated through a recurrent fuzzy neural network (RFNN). Finally, we present the numerical simulation results to illustrate the effectiveness of the ISSMC scheme. Also the chattering does not appear due to the actual control signal is obtained after an integrating operation.

The major contributions of this paper are: (1) the successful development of the ISSMC system for a chaotic tracking problem; (2) the successful development of the RFNN to confront the behavior of a chaotic system; (3) the successful derivation of parameter learning algorithms in the Lyapunov stabile theorem; (4) the successful derivation of the robust compensator with exponential reaching phase; (5) the successful application of the ISSMC system on a chaotic dynamic system with robust control performance and high accuracy response.

ACKNOWLEDGMENT

The authors appreciate the partial financial support from the National Science Council of Republic of China under grant NSC 102-2221-E-032-052.

REFERENCES

[1] Utkin, V.I., 1978. Sliding Modes and Theirs Applications in Variable Structure Systems. MIR Editors, Moscow.

[2] Huang, Y.J., Kuo, T.C., Chang, S.H., 2008. Adaptive sliding-mode control for nonlinear systems with uncertain parameters. IEEE Trans. Syst. Man Cybern. 38 (Pt-B), 534–539.

[3] Pisano, A., Davila, A., Fridman, L., Usai, E., 2008. Cascade control of PM DC drives via second-order sliding-mode technique. IEEE Trans. Ind. Electr. 55, 3846–3854.

[4] Bartolini, G., Pisano, A., Usai, E., 2009. On the second-order sliding mode control of nonlinear systems with uncertain control direction. Automatica 45, 2982–2985.

[5] Lin, F.J., Chen, S.Y., Huang, M.S., 2011. Adaptive complementary sliding-mode control with MIMO RHNN estimator for thrust active magnetic bearing system. Contr. Eng. Practice 19, 711–722.

[6] Sun, T., Pei, H., Pan, Y., Zhou, H., Zhang, C., 2011. Neural network-based sliding mode adaptive control for robot manipulators. Neurocomputing 74, 2377–2384.

[7] Lee, L.W., Li, I.H., 2012. Wavelet-based adaptive sliding-mode control with H^{∞} tracking performance for pneumatic servo system position tracking control. IET Control Theory Appl. 6, 1699–1714.

[8] Lin, C.M., Hsu, C.F., Chen, T.Y., 2012. Adaptive fuzzy total sliding-mode control of unknown nonlinear systems. Int. Journal of Fuzzy Syst. 14, 434–443.

[9] Kayacan, E., Kayacan, E., Ramon, H., Saeys, W., 2013. Adaptive neuro-fuzzy control of a spherical rolling robot using sliding-mode-control-theory-based online learning algorithm. IEEE Trans. Cybern. 43, 170–179.

[10] Hsu, C.F., 2013. Adaptive neural complementary sliding-mode control via functional-linked wavelet neural network. Eng. Appl. Artif. Intell. 26, 1221–1229.

[11] Hsu, C.F., Kuo, T.C., 2014. Adaptive exponential-reaching sliding-mode control for antilock braking systems. Nonlinear Dyn. 77, 993–1010.

[12] Lin, C.T., Lee, C.S.G., 1996. Neural Fuzzy Systems: A Neuro-Fuzzy Synergism to Intelligent Systems. Prentice-Hall, Englewood Cliffs, NJ.

[13] Wai, R.J., Shih, L.C., 2012. Adaptive fuzzy-neural-network design for voltage tracking control of a DC-DC boost converter. IEEE Trans. Power Electr. 27, 2104–2115.

[14] Theocharis, J.B., 2006. A high-order recurrent neuro-fuzzy system with internal dynamics: Application to the adaptive noise cancellation. Fuzzy Sets Syst., 157, 471–500.

[15] Juang, C.F., Chen, J.S., 2006. Water bath temperature control by a recurrent fuzzy controller and its FPGA implementation. IEEE Trans. Ind. Electr. 53, 941–949.

[16] Hsu, C.F., Cheng, K.H., 2008. Recurrent fuzzy-neural approach for nonlinear control using dynamic structure learning scheme. Neurocomputing 71, 3447–3459.

[17] Lin, F.J., Teng, L.T., Lin, J.W., Chen, S.Y., 2009. Recurrent FL-based fuzzy neural network controlled induction generator system using improved particle swarm optimization. IEEE Trans. Ind. Electr. 56, 1557–1577.

[18] Juang, C.F., Huang, R.B., Lin, Y.Y., 2009. A recurrent self-evolving interval type-2 fuzzy neural network for dynamic system processing, IEEE Trans. Fuzzy Syst. 17, 1092–1105.

[19] Chen, G., Dong, X., 1993. On feedback control of chaotic continuous-time systems. IEEE Trans. Circuits Syst. 40 (Pt-1), 591–601.

[20] Chen, C.H., Lin, C.M., Li, M.C., 2011. Development of PI training algorithm for neuro-wavelet control on synchronization of uncertain chaotic systems. Neurocomputing 74, 2797–2812.

[21] Hsu, C.F., 2014. Intelligent control of chaotic systems via self-organizing Hermite-polynomial-based neural network. Neurocomputing 123, 197–206.

[22] Lin, F.J., Hung, Y.C., Chen, S.Y., 2010. FPGA-based intelligent dynamic sliding-mode control using recurrent wavelet neural network for linear ultrasonic motor. IET Contr. Theory Appl. 4, 1511–1532.

[23] Tsai, J.Z., Hsu, C.F., Chiu, C.J., Peng, K.L., 2011. FPGA-based adaptive dynamic sliding-mode neural control for a BLDC motor. Asian J. Control 13, 845–857.

[24] El-Sousy, F.F.M., 2013. Adaptive dynamic sliding-mode control system using recurrent RBFN for high-performance induction motor servo drive. IEEE Trans. Ind. Informat. 9, 1922–1936.

[25] Slotine, J.J.E., Li, W.P., 1991. Applied Nonlinear Control. Prentice-Hall, Englewood Cliffs, NJ.

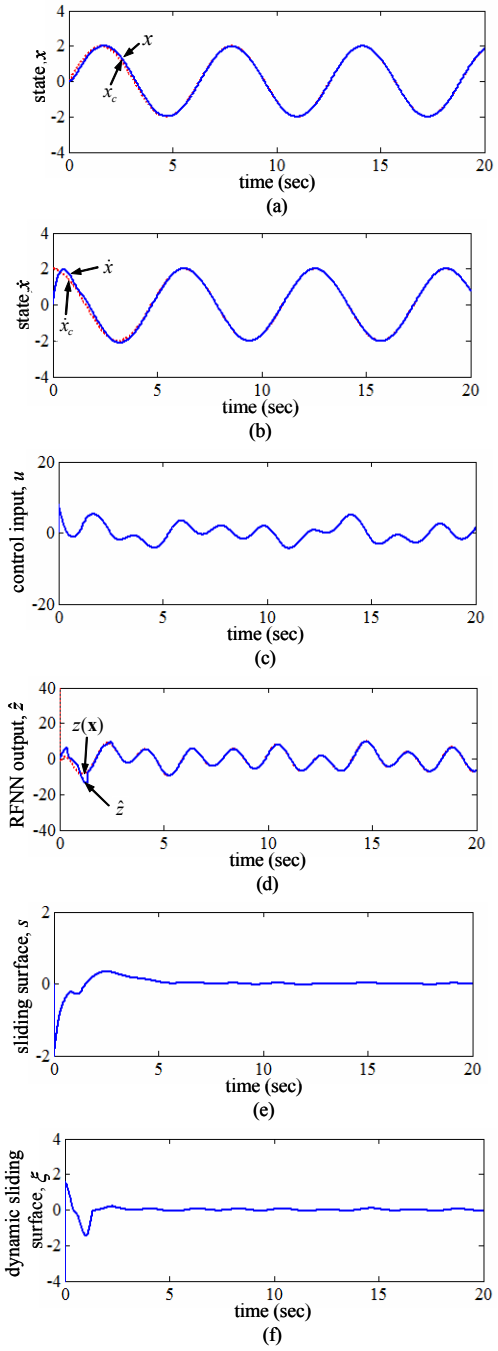

Fig. 4. Simulation results of chaotic dynamic for Case 1.
(a) the control response x
(b) the control response $\dot{x}$
(c) the control input u
(d) the RFNN output $\hat{z}$
(e) the sliding surface response s
(f) the dynamic sliding surface response ξ

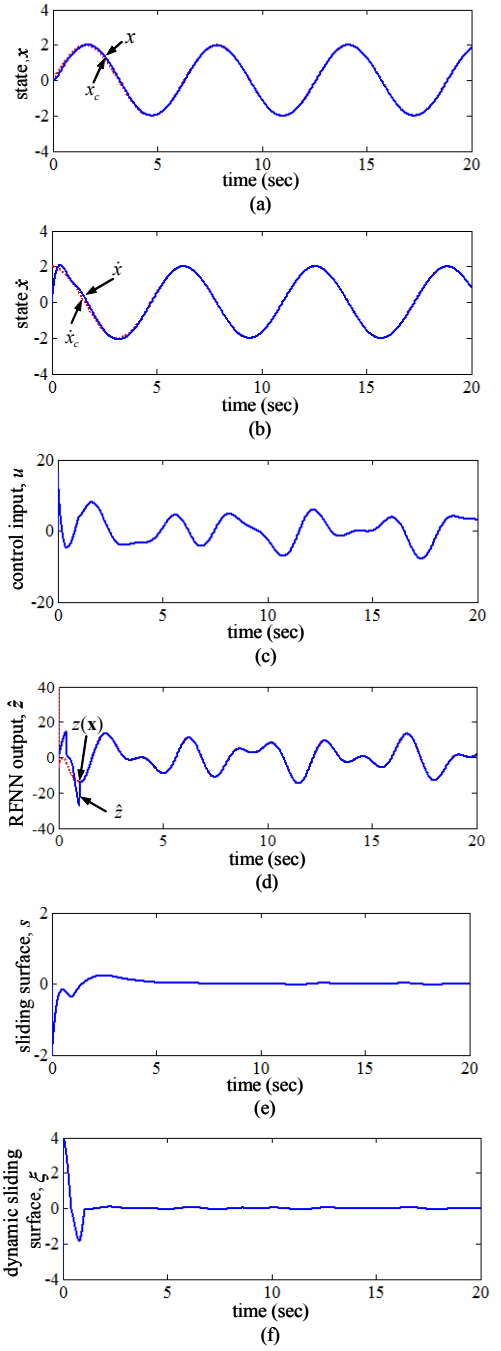

Fig. 4. Simulation results of chaotic dynamic for Case 1.
(a) the control response x
(b) the control response $\dot{x}$
(c) the control input u
(d) the RFNN output $\hat{z}$
(e) the sliding surface response s
(f) the dynamic sliding surface response ξ